Layer-by-layer assembled nanorough iridium-oxide/platinum-black for low-voltage microscale electrode neurostimulation

Shota Yamagiwa [a], Akifumi Fujishiro [a], Hirohito Sawahata [a], Rika Numano [b,c], Makoto Ishida [a,b], Takeshi Kawano [a,*]

[a] Department of Electrical and Electronic Information Engineering, Toyohashi University of Technology, Toyohashi 441-8580, Japan
[b] Electronics-Interdisciplinary Research Institute (EIIRIS), Toyohashi University of Technology, Toyohashi, Aichi 441-8580, Japan
[c] Department of Environmental and Life Sciences, Toyohashi University of Technology, Toyohashi, Aichi 441-8580, Japan

ARTICLE INFO

ABSTRACT

Electrical neural stimulating electrodes play an important role in medical applications and improving health/medical conditions. However, size reduction for low-invasive electrodes creates issues with high electrolyte/electrode interfacial impedance and low charge-injection characteristics, which makes it impossible to stimulate neurons/cells. To overcome these limitations, we propose an electrode material for low-voltage microscale electrode neurostimulation that combines the advantages of low impedance of iridium oxide (IrOx) with the enhanced surface area of platinum black (Pt-black). Based on a simple, rapid, low-temperature electroplating process, herein a low impedance and high charge-injection electrode is fabricated by a layer-by-layer assembly of IrOx/Pt-black with nanoscale roughness. The assembled nanorough-IrOx/Pt-black electrode has an impedance of $32\,\Omega\,cm^2$ at 1 kHz and a charge-injection delivery capacity (Q_{CDC}) of $46.7\,mC\,cm^{-2}$, which are 0.5 and 2.4 times the values for the same-sized IrOx/flat-Pt electrode, respectively. The stimulation capability of the nanorough-IrOx/Pt-black plated microelectrode is confirmed by *in vivo* stimulations of the sciatic nerve of a mouse. The threshold voltages of 8-μm-diameter and 11-μm-diameter electrodes are 700 mV and 300 mV, respectively. However, increasing the diameter of high Q_{CDC} nanorough-IrOx/Pt-black can further reduce the stimulation voltage. Consequently, nanorough-IrOx/Pt-black is applicable to low-voltage microscale electrode neurostimulations for powerful *in vivo/in vitro* electrophysiological measurements.

© 2014 Elsevier B.V. All rights reserved.

1. Introduction

Electrical neural stimulating electrodes, which play an important role in medical applications, have been used to improve medical conditions, including epilepsy, Parkinson disease [1], blindness [2], and hearing loss [3]. Recent advances in brain–machine interface (BMI) technology, which enables direct communications between the brain and external actuators [4,5], have realized a powerful neural stimulation application where tactile feedback occurs through microscale stimulation of the somatosensory cortex, or the so called brain–machine–brain interface (BMBI)

[6]. Conventional electrodes, which are composed of sharpened needle-like metal electrodes with diameters of several tens of microns or larger, are typically used in electrical stimulations of neurons/cells [7]. Although the needle-electrode diameter can be further reduced using recent microfabrication technology for low invasive electrodes and chronic device implantations [8–10], size reduction-induced issues such as high electrolyte/electrode interfacial impedance and low charge injection characteristics of the electrode remain problematic in high-performance microscale stimulations of neurons/cells [11]. Such size reduction-induced issues make it impossible for the electrode to stimulate the target neurons, as well as the recording [12]. Moreover, improving both the impedance and charge-injection characteristics of the electrode is important to reduce the stimulating voltages applied to the electrode in a biological sample such as a brain or nerve.

Candidate electrode materials to improve the electrode's electrical properties have been reported: Pt-black [13], titanium nitride (TiN) [14], IrOx [15], poly(3,4-ethylenedioxythiophene) (PEDOT) [11], and carbon nanotube (CNT) [16]. Pt-black can enhance the
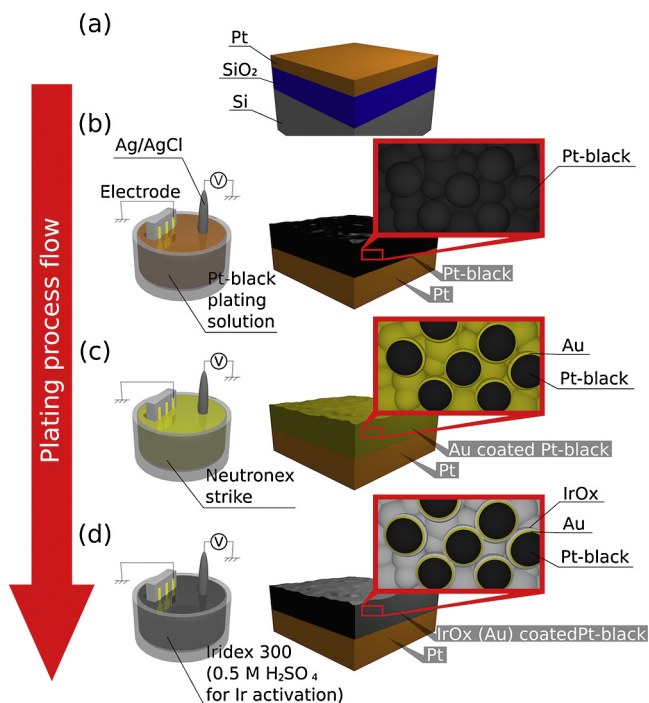
Fig. 1. Fabrication process steps for a nanorough-IrOx/Pt-black electrode: (a) initial flat-Pt platform electrode, (b) Pt-black plating over the Pt electrode, (c) Au plating as the adhesion layer, and (d) Ir plating and subsequent activation of the Ir for nanorough-IrOx/Pt-black.

effective surface area of Pt by creating nanoporous [13], and its mechanical stability has been demonstrated by penetrating the Pt-black tipped microneedle into a rat's cortex [9]. IrOx is a material with an excellent charge-injection delivery capacity (Q_{CDC}) (*e.g.*, 3.0 mC cm^{-2} for IrOx ≫ 0.075 mC cm^{-2} for Pt) [17]. Herein we combine these materials to develop low-impedance and high charge-injection electrodes *via* a layer-by-layer assembly of IrOx/Pt-black with nanoscale roughness based on electroplating, which is a simple, rapid, and low temperature (<60 °C) process. Hence, electrodes can be prepared on numerous device substrates, including silicon-microelectronics, flexible thin films, and three-dimensional micro/nanoelectromechanical systems (MEMS, NEMS) [8,9].

2. Methods

Nanorough-IrOx/Pt-black electrodes were fabricated by a layer-by-layer nanoscale assembly technique. Of the three layers, the first layer of Pt-black was used as a nanoporous template to enhance the effective electrode area [13], while the second gold (Au) layer improved the interfacial adhesion between Pt-black and the subsequent Ir layer. The third layer of IrOx was used to improve Q_{CDC} of the electrode [15].

Fabrication was based on a simple, rapid, low-temperature electroplating process. The first layer of Pt-black was electroplated with a Pt chloride solution (10 g $H_2PtCl_6 \cdot 6H_2O$, 0.1 g $Pb(CH_3COO)_2 \cdot 3H_2O$, and 300 ml deionized water (DIW) at room temperature) [13]. For a 100-nm thick Pt-black, the plating direct-current (DC) bias was 400 mV with a plating time of 10 s (Fig. 1b). After forming an Au adhesive layer at 32 °C (Neutronex Strike Au, Tanaka Holdings Co., Ltd.) (Fig. 1c), an ~10-nm-thick Ir layer was electroplated with an Ir solution (Iridex-300, Tanaka Holdings Co., Ltd.) at a 700-mV DC bias for 2 min and a plating temperature of 60 °C (Fig. 1d). Then Ir activation was achieved in a 0.5 M H_2SO_4

solution (room temperature). To avoid filling the nanoporous template of Pt-black with Au and Ir, thicknesses of the Au and Ir were limited to ~10 nm and ~10 nm, respectively. To activate Ir, we used triangle wave signals (+600 mV for high and −200 mV for low levels) at 100 mV s^{-1} for 2300 cycles. Fig. 2a shows a fabricated millimeter-scale nanorough-IrOx/Pt-black electrode array using platform 0.5-mm × 1.5-mm flat-Pt electrodes. Fig. 2b shows a microscale nanorough-IrOx/Pt-black electrode fabricated using an 8-μm-diameter flat-Pt electrode.

3. Results and discussion

Nanorough-IrOx/Pt-black electrodes can be assembled on Pt electrodes with numerous patterns (Fig. 2a and b). The atomic force microscope (AFM) image shows that the enhanced surface roughness of the IrOx/Pt-black electrode is due to the first layer of Pt-black (Fig. 2d). The roughness of IrOx/Pt-black is larger than other IrOx layers formed on a flat-Pt electrode using the same plating process without forming Pt-black (Fig. 2c). The transmission electron microscope (TEM) image of IrOx/Pt-black confirms that the observed roughness in the AFM image is consistent with the cross-sectional structure of the electrode with a similar roughness of ~100 nm (Fig. 2e).

The electrical properties of the fabricated nanorough-IrOx/Pt-black electrode were measured in saline. For microscale electrode measurements, size reduction-induced effects such as the spreading resistance of the electrode [18] and parasitic impedance of the device interconnection [12] should be eliminated in order to obtain size-independent properties of a nanorough-IrOx/Pt-black electrode. Thus, we investigated a millimeter-scaled electrode (0.5 mm × 1.5 mm, Fig. 2a).

To obtain the impedance shifts during the plating processes, herein step-by-step impedances for Pt, Pt-black, nanorough-Ir/Pt-black, and nanorough-IrOx/Pt-black were measured. Note that "nanorough-Ir/Pt-black" indicates a nanorough-Ir/Pt-black electrode before Ir activation. The electrode impedance was measured in a room temperature 0.9% NaCl saline solution bath with a sinusoidal wave (200 mV$_{p-p}$ amplitude, 3×10^{-3} Hz–1 MHz) applied *via* a silver−silver chloride (Ag−AgCl) counter electrode. An impedance analyzer (Model 1260A Impedance/Gain-Phase Analyzer, AMETIC, Inc) was used in all impedance measurements. The step-by-step measurements clearly demonstrate a reduced electrode impedance. Compared to the initial Pt layer and the first layer of the Pt-black electrode, nanorough-IrOx/Pt-black has a 40-fold and 2-fold lower impedance at 1 kHz, respectively (Fig. 3a). The calculated impedance of nanorough-IrOx/Pt-black per unit area was 32 Ω cm^2 at 1 kHz. In the frequency range of 1–100 Hz, the electrode shifts from the capacitive phase to the resistive phase after Pt-black electroplating during the impedance measurements (Fig. 3b). The maximum resistive-phase angle in this electrode process occurs after IrOx formation by Ir activation. In a frequency range of 10^{-3}–1 Hz, nanorough-IrOx/Pt-black and flat-IrOx/Pt exhibit further capacitive phases compared to nanorough-Ir/Pt-black and Pt-black. This phase difference is due to the increased constant phase element (CPE) and the decreased interfacial resistance after IrOx formation by Ir activation [19].

To investigate the change in Q_{CDC} for different electrodes (Pt, Pt-black, nanorough-Ir/Pt-black, and nanorough-IrOx/Pt-black), we measured the step-by-step cyclic voltammogram (CV) responses. The electrodes were placed in the same saline bath, and swept from −0.85 to 0.9 V for Pt and Pt-black, and from −0.9 to 1 V for nanorough-Ir/Pt-black, nanorough-IrOx/Pt-black, and IrOx/flat-Pt at a constant sweep rate of 100 mV s^{-1} *versus* a Ag−AgCl reference electrode and a Pt counter electrode. Each CV response was
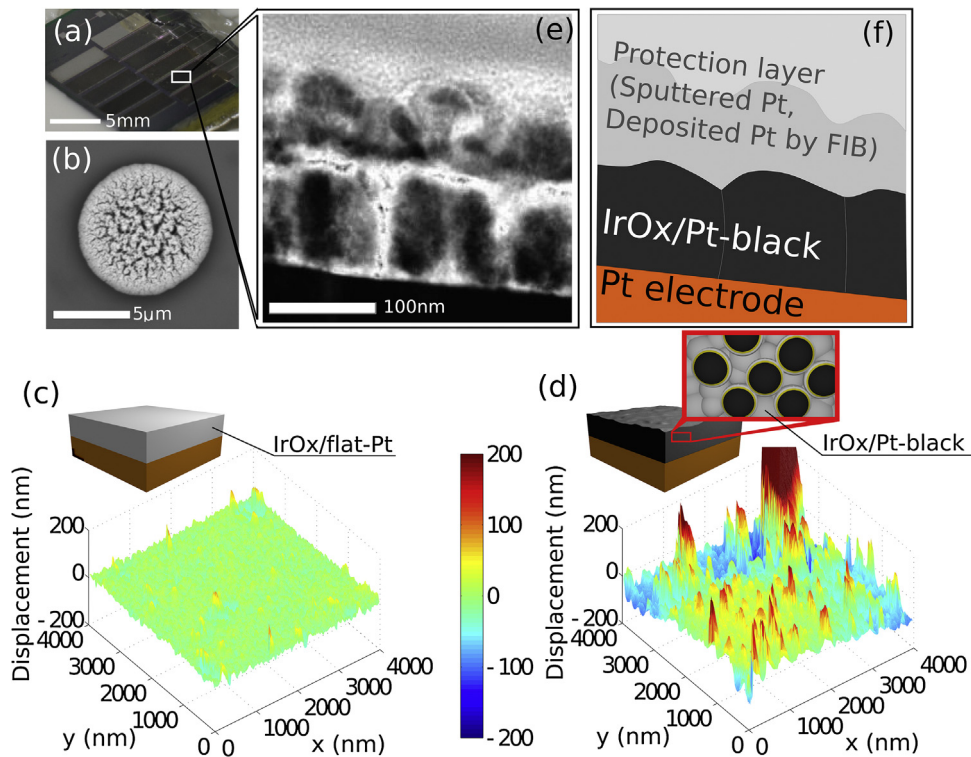
Fig. 2. Nanorough-IrOx/Pt-black electrodes. (a) Photograph of a 0.5-mm × 1.5-mm electrode array and (b) top-view SEM image of an 8-μm-diameter electrode. AFM images of the surface morphologies taken from (c) a IrOx/flat-Pt template and (d) a nanorough-IrOx/Pt-black template. (e) Cross-sectional TEM image of the electrode taken from the device shown in (a). (f) Schematic of the TEM image in (e) where the protection layer is sputtered Pt.

the average of five measurements. The CV responses of the step-by-step measurements indicate that the charge transfer increases (Fig. 3c). The calculated Q_{CDC} of Pt and Pt-black are 3.8 mC cm^{-2} and 24.0 mC cm^{-2}, respectively, whereas those of nanorough-Ir/Pt-black and nanorough-IrOx/Pt-black are 52.7 mC cm^{-2} and 46.7 mC cm^{-2}, respectively. These values are 2.4 times higher than that of IrOx/flat-Pt (19.4 mC cm^{-2}) (Fig. 3d).

Compared to a same-size conventional electrode (*e.g.*, Pt-black and IrOx/flat-Pt), the nanorough-IrOx/Pt-black electrode exhibits lower impedance and higher Q_{CDC} characteristics. The lower impedance can improve both the neural stimulation and recording capabilities of the electrode, especially for an electrode with a small recording area such as micro/nanoscale electrodes. Because a stimulating voltage is applied to the neural stimulating electrode in a biological sample, lower voltages are important in terms of safety [20] and low power consumption. Previous experimental reports on a ~1300-nm-thick IrOx show higher current densities with peaks at −200 and +400 mV [15]. Our nanorough-Ir/Pt-black exhibits similar CV characteristics, but nanorough-IrOx/Pt-black and nanorough-Ir/Pt-black do not exhibit significant differences between voltages of −600 mV to +600 mV, probably due to the thin layer of the assembled IrOx (<10 nm). The Ir oxidation of nanorough-Ir/Pt-black before the Ir activation process is another reason for the similar CV characteristics. Several parts of Ir over Pt-black might be oxidized during the impedance and CV measurements in saline, resulting in different Ir electrical properties from the as-assembled Ir. Note that amplitudes used in impedance and CV measurements of Ir were ±200 mV and −0.9–1 V, respectively.

The current waveform was observed with nanorough-Ir/Pt-black tipped microneedle (diameter: ~8 μm) electrode in saline. The microscale diameter needle electrode array with the length of 120 μm was prepared by a silicon-wire growth technique and subsequent microfabrication processes [9]. To demonstrate the possibility of the stimulation with the microelectrode, the current waveforms in response to a biphasic voltage pulse were observed in saline (Fig. 3e and f). The voltage pulse with the amplitude of ±200 mV was applied to the microneedle electrode in saline at room temperature. The peak values of the observed currents exhibited 40 μA for Pt-black tipped and 98 μA for nanorough-Ir/Pt-black tipped microneedle electrodes, respectively, indicating that nanorough-Ir/Pt-black electrode can make larger currents than that of Pt-black in saline with the same voltage pulse.

To confirm that charge injection characteristics of the proposed nanorough-IrOx/Pt-black electrode is sufficient for neural stimulation, *in vivo* animal experiments were performed. With the proposed plating steps (Fig. 1), we prepared an array of 8-μm-diameter nanorough-IrOx/Pt-black electrodes [electrode impedance = 1.39 ± 0.65 MΩ to 27.92 ± 5.44 kΩ (mean ± std.) for 10 Hz to 10 kHz] spaced at 420-μm intervals (Fig. 4c). The nanorough-IrOx/Pt-black microelectrode array was fabricated on Pt electrodes with an insulating layer of parylene (1 μm in thickness) (Fig. 4d and e). The stimulation capability of the microelectrode was demonstrated *via* electrical stimulation of the sciatic nerve in three mice (18–31 g-weight). The mice were deeply anesthetized with urethane (50 μl of 30% solution/10 g body weight). The fabricated electrode device was placed underneath a mouse's sciatic nerve, while each electrode was in contact with the nerve (Fig. 4a and b). For electrical stimulation of the nerve, the electrodes were connected to an isolator (Tucker Davis Technology Inc., IZ2). The evoked electromyogram (EMG) signals of the mouse's muscle were detected through two wire electrodes (0.1-mm-diameter metal wires), which were connected to an amplification system (Tucker Davis Technology Inc., SH16: headamplifier and PZ2: preamplifier). Forceps, which clamped the mouse's skin, served as the reference electrode for the stimulation. In all stimulations, 50-ms-duration biphasic voltage pulses with an amplitude ranging from 500 to 900 mV were applied to the nerve *via* the 8-μm-diameter nanorough-IrOx/Pt-black microelectrode (Fig. 4f). All
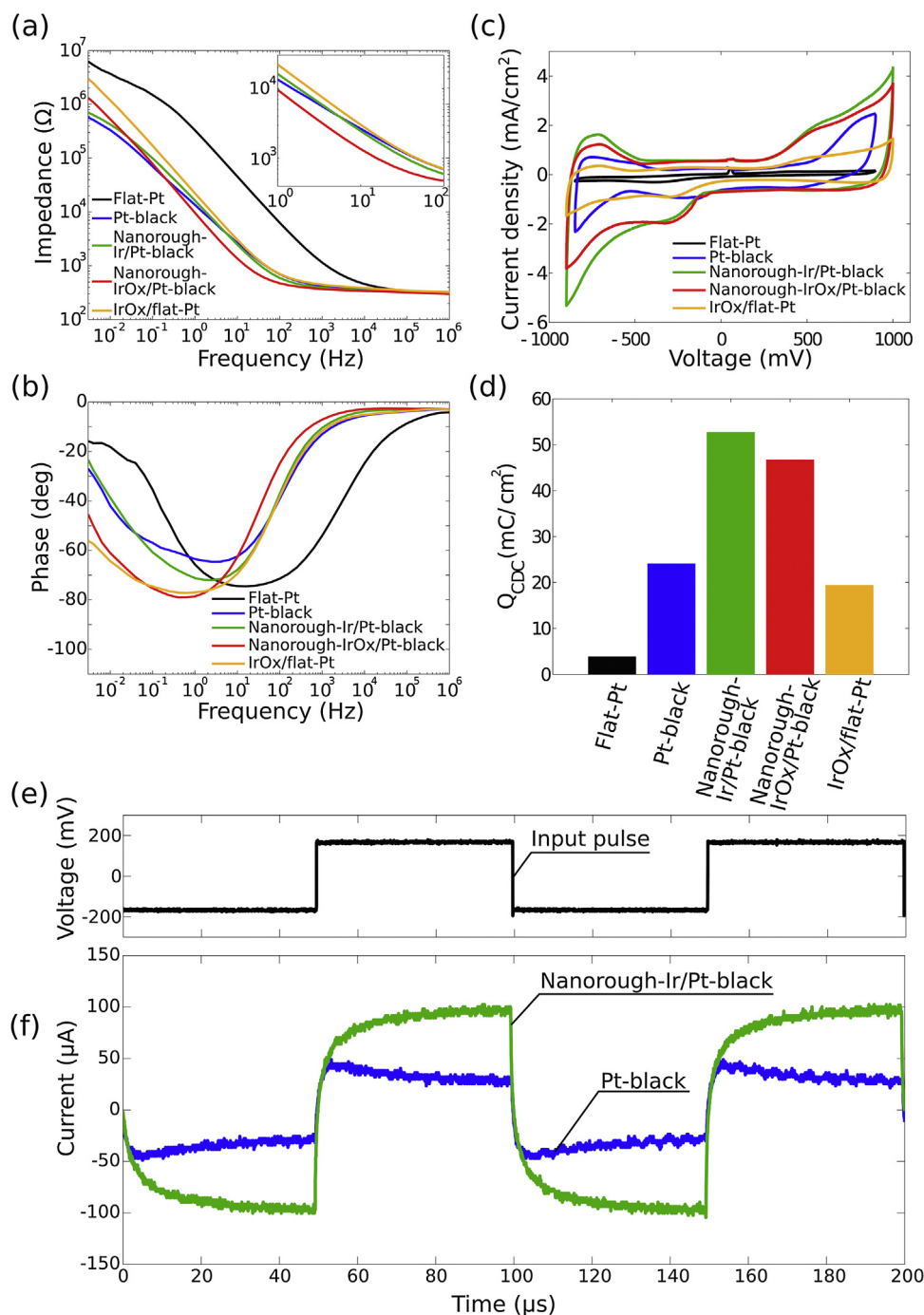
Fig. 3. Electrical properties of each electrode material. (a) Impedance shifts, (b) phase shifts, and (c) cyclic voltammogram shifts of the 0.5 × 1.5-mm electrode observed by measuring the step-by-step electrical properties. (d) Changes in Q_{CDC} obtained from the CV responses of the electrodes. IrOx/flat-Pt electrode is included for comparison. (e, f) A current transient of nanorough-Ir/Pt-black tipped microneedle electrode in response to a biphasic voltage pulse. For comparison, the graph also includes the current transient of Pt-black tipped microneedle electrode. The diameter of the microneedle electrode was 8 μm.

experimental procedures and animal care were approved by the animal experiments committee of Toyohashi University of Technology.

Animal experiments confirm that the nanorough-IrOx/Pt-black microelectrode stimulates the sciatic nerve of the mouse with a voltage, which is low enough potential to prevent the electrolysis (e.g., <1 V). The EMG waveforms during nerve stimulation ranged from 500 to 800 mV are observed (Fig. 4f–h). The EMG signals exhibit small amplitudes for stimulation amplitudes of 500 and 600 mV (left two panels in Fig. 4g and h), but large amplitudes for stimulation amplitudes greater than 700 mV (right two

panels in Fig. 4g and h). Additionally, stimulation amplitudes above 700 mV cause movement of the mouse's leg. The EMG amplitude depends on the stimulation voltage with the threshold voltage of 700 mV (8-μm-diameter nanorough-IrOx/Pt-black electrodes, in Fig. 5). Herein we used a normalized EMG value of two, which is double the amplitude of noise, to determine the stimulation threshold voltage for all trials. These results indicate that the threshold voltage for electrical stimulation is about 700 mV, which is low enough to prevent electrolysis of water in a biological sample.

Although the neural stimulation capability is demonstrated using sciatic nerves of mice, the spatial alignment between the
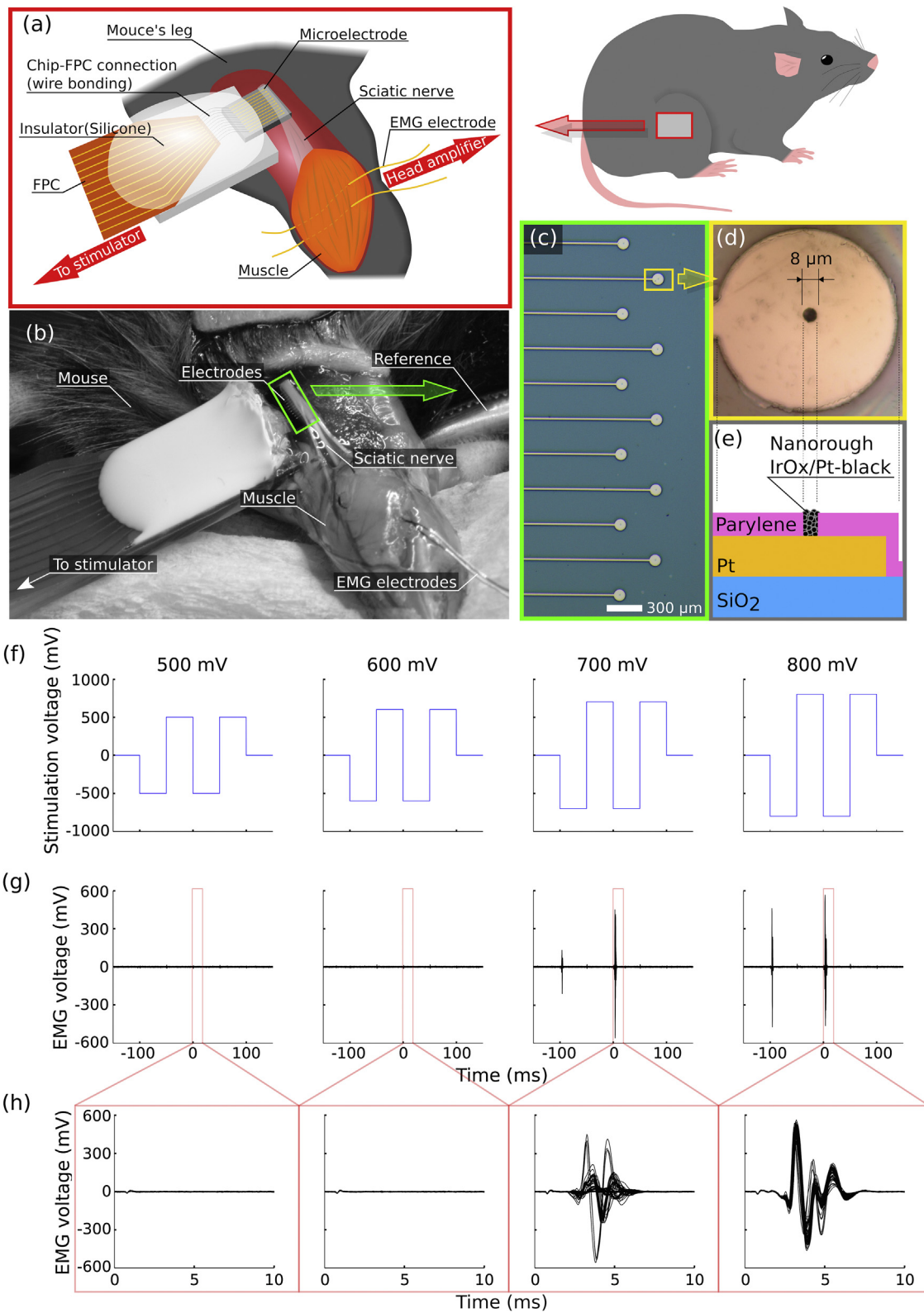
Fig. 4. *In vivo* neural stimulation with a 8-µm-diameter nanorough-IrOx/Pt-black electrode array. (a) Schematic image and (b) photograph showing preparations for the stimulation where the fabricated microelectrode array chip is placed underneath the mouse's sciatic nerve. (c) Microscope image of an array of fabricated microelectrodes. Diameter of the nanorough-IrOx/Pt-black electrode is 8 µm and the spacing between electrodes is 420 µm. (d) Photograph of an individual microelectrode. (e) Schematic cross-sectional image of the microelectrode. (f) Biphasic voltage pulses (50-ms duration, 500–800-mV amplitudes) applied to the nerve *via* the nanorough-IrOx/Pt-black microelectrode. (g) Recorded EMG signals during the stimulation of the sciatic nerve filtered with a 500 Hz to 3 kHz bandpass. (h) Enlarged waveforms of the EMG signals. These superimposed waveforms of EMG signals are from 30 stimulation trials using a mouse.
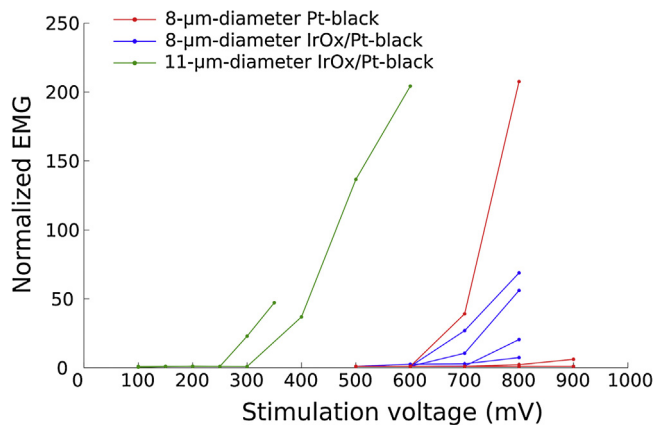
Fig. 5. Stimulation voltage-dependent EMG amplitudes. These normalized EMG signals are given by the ratio of EMG and noise amplitudes [normalized EMG = root-mean-square (rms) EMG amplitude/rms noise amplitude]. Graph includes EMGs evoked by 8-μm-diameter Pt-black (red), 8-μm-diameter nanorough-IrOx/Pt-black (blue), and 11-μm-diameter nanorough-IrOx/Pt-black (green) electrodes. (For interpretation of the references to color in this figure legend, the reader is referred to the web version of the article.)

microscale electrode and the sciatic nerve (∼1 mm in diameter) is essential. The threshold voltage varies between nanorough-IrOx/Pt-black electrodes with the same diameter (8-μm-diameter nanorough-IrOx/Pt-black electrodes, in Fig. 5), which may be because the microscale electrode allows a limited area within a biological tissue to be stimulated compared to that using a conventional electrode with a larger diameter (several tens micrometers or more). In addition, variations are also observed in the stimulations using a Pt-black microelectrode with the same diameter (8-μm-diameter Pt-black electrodes, in Fig. 5). Three of five trials *via* the Pt-black electrode exhibit threshold voltages above 900 mV, while one trial exhibits a threshold voltage of 700 mV. Due to the microscale diameter electrode (8 μm), this difference in the threshold voltage between trials is probably due to an alignment shift because the microelectrode position was manually controlled in each trial. In addition to the alignment issue, it is necessary to discuss the different charge injection mechanism between materials: Fardaic reaction for IrOx, and both Fardaic reaction and capacitive (pseudocapacitive) for Pt [14]. The different stimulation mechanism might also affect the effective charges for the stimulation; further discussions including the alignment issue are required and will be reported in future literature.

Increasing the diameter of the nanorough-IrOx/Pt-black microelectrode decreases the stimulation threshold voltage. Due to the higher charge injection characteristics of the 11-μm-diameter nanorough-IrOx/Pt-black compared to that of the 8-μm-diameter electrode (Q_{CDC} of 46.7 mC cm^{-2} as shown in Fig. 3d), the 11-μm-diameter electrode exhibits a threshold voltage less than 300 mV (Fig. 5), which is half the threshold voltage of the 8-μm-diameter electrode. Note that the stimulations were demonstrated using two mice, whereas the stimulations with the 8-μm-diameter electrodes (8 μm-diameter nanorough-IrOx/Pt-black electrodes, in Fig. 5) used one mouse. Such a high Q_{CDC} of nanorough-IrOx/Pt-black (46.7 mC cm^{-2} in Fig. 3d) suggests that increasing the diameter of the nanorough-IrOx/Pt-black electrode (>11-μm diameter) may realize even lower stimulation voltages (<300 mV). A lower simulation voltage is an important characteristic of a neural stimulation electrode, in terms of safety in a biological sample, long term stability of the electrode (*e.g.*, insulating layer), and the electrode integration with on-chip microelectronics as a neural stimulation microsystem.

4. Conclusion

In summary, we propose and demonstrate electrodes with low impedance and high charge-injection characteristics based on a layer-by-layer assembly of IrOx/Pt-black with nanoscale roughness for low-voltage microelectrode stimulation. Enhancing the surface roughness of IrOx with an underneath nanoporous template of Pt-black improves the charge-injection characteristics of IrOx/flat-template, resulting in a higher Q_{CDC} than that of the IrOx/flat-template. Because the electrode process is based on a simple, rapid, and low temperature (<60 °C) electroplating process, it can be applied to numerous device substrates, including silicon-microelectronics, flexible thin films, and MEMS/NEMS. The charge injection of the nanorough-IrOx/Pt-black plated microscale electrodes is sufficient for electrophysiological neural stimulations, as demonstrated by the low voltage stimulation (<1 V) of sciatic nerves of mice *in vivo*. Although we demonstrated the stimulation using the sciatic nerve of a mouse, stimulating microelectrodes with diameters of <11 μm can be used for *in vivo/in vitro* stimulation of individual neurons in which the cell body (soma) has a similar diameter (∼10 μm). In the future, we plan to realize high-density microelectrode arrays of the nanorough-IrOx/Pt-black for high spatial resolutions of neural stimulations. Such low impedance characteristics of the electrode material should also offer high-performance neuronal recording micro/nanoscale electrodes. In addition to electrophysiological measurements, the nanorough-IrOx/Pt-black electrodes are applicable to numerous other sensor applications, including high-performance chemical sensors and gas sensors [21,22].

References

[1] P.S. Motta, J.W. Judy, IEEE Trans. Biomed. Eng. 5 (2005) 923–933.
[2] E. Zrenner, K.U. Bartz-Schmidt, H. Benav, D. Besch, A. Bruckmann, V.P. Gabel, F. Gekeler, U. Greppmair, A. Harscher, S. Kibbel, J. Koch, A. Kusnyerik, T. Peters, K. Stingl, H. Sachs, A. Stett, P. Szurman, B. Wilhelm, R. Wilke, Proc. R. Soc. B 3 (2011) 1489–1497.
[3] F.G. Zeng, Trends Amplif. 1 (2004) 1–34.
[4] L.R. Hochberg, M.D. Serruya, G.M. Friehs, J.A. Mukand, M. Saleh, A.H. Caplan, A. Branner, D. Chen, R.D. Penn, J.P. Donoghue, Nature 442 (2006) 164–171.
[5] L.R. Hochberg, D. Bacher, B. Jarosiewicz, N.Y. Masse, J.D. Simeral, J. Vogel, S. Haddadin, J. Liu, S.S. Cash, P. Smagt, P. Donoghue, Nature 485 (2012) 372–377.
[6] J.E. O'Doherty, M.A. Lebedev, P.J. Ifft, K.Z. Zhuang, S. Shokur, H. Bleuler, M.A.L. Nicolelis, Nature 479 (2011) 228–231.
[7] S. Kim, R. Bhandari, M. Klein, S. Negi, L. Rieth, P. Tathireddy, M. Toepper, H. Oppermann, F. Solzbacher, Biomed. Microdevices 11 (2009) 453–466.
[8] D.H. Szarowski, M.D. Andersen, S. Retterer, A.J. Spence, M. Isaacson, H.G. Craighead, J.N. Turner, W. Shain, Brain Res. 983 (2003) 23–35.
[9] A. Fujishiro, H. Kaneko, T. Kawashima, M. Ishida, T. Kawano, Sci. Rep. 4 (4868) (2014).
[10] D. Takashi, K. Yoshida, B.L. Nicholas, R.P. Paras, D. Xiaopei, Z. Huanan, L.S. Karen, L. Joerg, A.K. Nicholas, R.K. Daryl, Nat. Mater. 11 (2012) 1065–1073.
[11] M.R. Abidian, D.C. Martin, Adv. Funct. Mater. 4 (2009) 573–585.
[12] T. Harimoto, K. Takei, T. Kawano, A. Ishihara, T. Kawashima, H. Kaneko, M. Ishida, S. Usui, Biosens. Bioelectron. 5 (2011) 2368–2375.
[13] H. Oka, K. Shimono, R. Ogawa, H. Sugihara, M. Taketani, J. Neurosci. Methods 1 (1999) 61–67.
[14] S.F. Cogan, Annu. Rev. Biomed. Eng. (2008) 275–309.
[15] S.F. Cogan, J. Ehrlich, T.D. Plante, A. Smirnov, D.B. Shire, M. Gingerich, J.F. Rizzo, J. Biomed. Mater. Res. B: Appl. Biomater. 2 (2009) 353–361.
[16] E.W. Keefer, B.R. Botterman, M.I. Romero, A.F. Rossi, G.W. Gross, Nat. Nanotechnol. 3 (2008) 434–439.
[17] K.W. Horch, G.S. Dhillon, Bioengineering and Biomedical Engineering, University of Utah, World Scientific, United States, 2004, pp. 497.
[18] D.A. Robinson, Proc. IEEE 6 (1968) 1065–1071.

[19] X.T. Cui, D.D. Zhou, IEEE Trans. Neural Syst. Rehabil. Eng. 4 (2007) 502–508.
[20] Y. Lu, Z. Cai, Y. Cao, H. Yang, Y.Y. Duan, Electrochem. Commun. 5 (2008) 778–782.
[21] H. Wen-Ding, J. Wang, A. Thermpon, M. Chiao, J.C. Chiao, Proc. SPIE 6931 (2008) 693104.1–693104.9.
[22] E. Varkaraki, J. Nicole, E. Plattner, C.H. Comninellis, C.G. Vayenas, J. Appl. Electrochem. 25 (1995) 978–981.

Biographies

Shota Yamagiwa completed his B.S. degree in 2010 and M.S. degree in 2012 from the Department of Electrical and Electronic Engineering, Toyohashi University of Technology, Japan. He is pursuing his Ph.D. from the same institution.

Akifumi Fujishiro completed his M.S degree from Department of Electrical and Electronic Information Engineering, Toyohashi University of Technology, Japan, and he is currently pursuing Ph.D. from the same institution.

Hirohito Sawahata had been a Postdoctoral Research Fellow during 2009–2012 at Graduate school of Medical and Dental sciences, Niigata University, Japan and completed his Ph.D. from Graduate School of Science and Engineering, Yamagata University, Japan. During 2012–2013 he worked as an Assistant Professor at Graduate School of Medical and Dental sciences, Niigata University, Japan. Later on from 2013, he is working as an Assistant Professor, Department of Electrical and Electronic Information Engineering, Toyohashi University of Technology, Japan.

Rika Numano completed her B.Sc. in 1996, M.Sc. in 1998, and Ph.D. in 2002, all from Faculty of Technology, University of Tokyo, Japan. She was a Postdoctoral Research Fellow (Japan Society for the Promotion of Science), Human Genome Center Institute of Medical Science, University of Tokyo, Japan between 2002 and 2005, Postdoctoral Fellow (Japan Society for the Promotion of Science Postdoctoral fellowship for research abroad), Department of Molecular and Cell Biology, University of California Berkeley between 2005 and 2006, a researcher, Cell Function Dynamics, RIKEN between 2006 and 2007, a Researcher, ERATO Project, Japan Science and Technology Agency between 2007 and 2009 and Tenure-truck Associate professor, Electronics-Inspired Interdisciplinary Research Institute (EIIRIS), Toyohashi University of Technology, between 2009 and 2013. Currently, from 2013, she is working as an Associate professor, at Department of Environmental and Life Sciences, Toyohashi University of Technology, Japan.

Makoto Ishida completed his Ph.D. degree, Electronics Engineering, Kyoto University, Japan and was a Research Assistant, Department of Electric and Electronic Engineering, Toyohashi University of Technology, Japan. From 1997, he was a Professor, Electrical and Electronic Engineering, Toyohashi University of Technology, Japan. Besides, from 2008, he is Vice president on Research Affairs, Toyohashi University of Technology, Japan and from 2010 and still continuing as Director, Electronics Inspired-Interdisciplinary Research Institute (EIIRIS), Toyohashi University of Technology.

Takeshi Kawano completed his M.S. degree in 2001, Ph.D. degree in 2004, and between 2004 and 2005, he was a Postdoctoral Research Fellow at Department of Electrical and Electronic Engineering, Toyohashi University of Technology, Japan. During 2005–2007, he was a Postdoctoral Research Fellow (Japan Society for the Promotion of Science Postdoctoral fellowship for research abroad), Department of Mechanical Engineering, Berkeley Sensor and Actuator Center (BSAC), University of California Berkeley. During 2007–2010 was an Assistant Professor, Toyohashi University of Technology, Electrical and Electronic Engineering, Japan. From 2010 onwards he has been PRESTO Researcher, Japan Science and Technology Agency (JST) as well as an Associate Professor, Electrical and Electronic Information Engineering Toyohashi University of Technology, Japan.